2015

Cell Stimulation and Calcium Mobilization by Picosecond Electric Pulses

Iurii Semenov
Old Dominion University, isemenov@odu.edu

Shu Xiao
Old Dominion University, sxiao@odu.edu

Dongkoo Kang
Old Dominion University

Karl H. Schoenbach
Old Dominion University, kschoenb@odu.edu

Andrei G. Pakhomov
Old Dominion University, apakhomo@odu.edu

Original Publication Citation

Semenov, I., Xiao, S., Kang, D., Schoenbach, K. H., & Pakhomov, A. G. (2015). Cell stimulation and calcium mobilization by picosecond electric pulses. *Bioelectrochemistry, 105*, 65-71. doi:10.1016/j.bioelechem.2015.05.013

HHS Public Access

Author manuscript

Bioelectrochemistry. Author manuscript; available in PMC 2016 October 01.

Published in final edited form as:

Bioelectrochemistry. 2015 October ; 105: 65–71. doi:10.1016/j.bioelechem.2015.05.013.

Cell stimulation and calcium mobilization by picosecond electric pulses

Iurii Semenov[a,#], **Shu Xiao**[a,b,#], **Dongkoo Kang**[a,b], **Karl H. Schoenbach**[a], and **Andrei G. Pakhomov**[a,*]

[a]Frank Reidy Research Center for Bioelectrics, Old Dominion University, Norfolk, VA, USA

[b]Department of Electrical and Computer Engineering, Old Dominion University, Norfolk, VA, USA

Abstract

We tested if picosecond electric pulses (psEP; 190 kV/cm, 500 ps at 50% height), which are much shorter than channel activation time, can activate voltage-gated (VG) channels. Cytosolic Ca^{2+} was monitored by Fura-2 ratiometric imaging in GH3 and NG108 cells (which express multiple types of VG calcium channels, VGCC), and in CHO cells (which express no VGCC). Trains of up to 100 psEP at 1 kHz elicited no response in CHO cells. However, even a single psEP significantly increased Ca^{2+} in both GH3 (by 114+/−48 nM) and NG108 cells (by 6 +/−1.1 nM). Trains of 100 psEP amplified the response to 379+/−33 nM and 719+/−315 nM, respectively. Ca^{2+} responses peaked within 2–15 s and recovered for over 100 s; they were 80–100% inhibited by verapamil and ω-conotoxin, but not by the substitution of Na^{+} with N-methyl-D-glucamine. There was no response to psEP in Ca^{2+}-free medium, but adding external Ca^{2+} even 10 s later evoked Ca^{2+} response. We conclude that electrical stimuli as short as 500 ps can cause long-lasting opening of VGCC by a mechanism which does not involve conventional electroporation, heating (which was under 0.06 °K per psEP), or membrane depolarization by opening of VG Na^{+} channels.

Keywords

electrostimulation; picosecond pulses; calcium; membrane; electroporation

1. Introduction

Externally applied pulsed electric fields have long been the most versatile tool for multi-scale control of biological systems. For conventional milli- and microsecond electric pulses (EP), two key events determine the whole spectrum of physiological effects: (1) activation of voltage-sensitive channels and (2) at higher amplitudes, permeabilization of cell membrane by electroporation[1, 2]. A recent expansion into the nanosecond EP range

*Corresponding author: Andrei G. Pakhomov, Frank Reidy Research Center for Bioelectrics, 4211 Monarch Way, Suite 300, Old Dominion University, Norfolk, VA 23508, USA, +1(210)2049012, +1(757)6838003, Fax: +1(757)4511010, apakhomo@odu.edu, 2andrei@pakhomov.net.

#equal contributions to the work

(nsEP) has enabled new tools such as nanoporation, permeabilization of organelles, and bipolar pulse cancellation [2–8]. Further advancement towards picosecond EP (psEP) treatments is technically challenging but brings a promise of a remote but localized electrostimulation by replacing the stimulation electrodes with broadband antennas [9, 10]. However, it is not known whether psEP stimulation is possible at all: It may require prohibitively high pulse amplitudes, and, even at highest amplitudes, it is not clear if excitation can be evoked by stimuli 5–6 orders of magnitude faster than the activation time of voltage-gated Na^+ and Ca^{2+} channels[11, 12].

Stimulatory effects have been shown for nano- but not picosecond EP. Several studies reported that a single high-amplitude stimulus of 350- 100-, 12-, 5-, 4-, and even 1-ns duration can activate nerve, muscle, and endocrine cells [13–18]. The thresholds varied for the different targets, but overall they expectedly became higher for shorter stimuli. The electric field of 24 kV/cm was required to excite frog neuromuscular preparation with a single 1-ns pulse [15]. However, high-rate nsEP trains could elicit action potentials even at low amplitudes. For example, delivering 12-ns pulses in 25 ms, 4 kHz bursts reduced the threshold for isolated nociceptor neurons from 0.4 to 0.016 kV/cm [13].

The authors argued that the mechanism of action potential generation in neurons [13] and in the neuromuscular preparation [15] was not different from the conventional electrostimulation with longer EP and did not involve electroporation. However, the absence of electroporation was either just a conjecture from the fact that the threshold for 1-ns stimuli fell roughly on the same strength-duration curve as the data for longer pulses [15], or was based on the lack of the uptake of propidium iodide [13] (which is not a sensitive marker of nanoporation [19, 20]). Ca^{2+} mobilization in cardiomyocytes by 4-ns EP was supposedly a mixed effect of conventional electrostimulation and the loss of the transmembrane potential (TMP) due to nanoporation [16]. In bovine chromaffin cells, Ca^{2+} mobilization by a single 5-ns, 50 kV/cm EP required opening of L-type voltage-gated calcium channels (VGCC) which was dependent on the tetrodotoxin-insensitive Na^+ uptake, possibly also due to nanoporation [17]. In other studies, nanoporation was achieved by a single 10-ns EP at about 40 kV/cm [21] or 120 kV/cm [22], or by trains of 3- or 4-ns EP at 40 kV/cm [23]. The estimated maximum temperature rise (see section 2.4 below) from the above EP treatments ranged from 0.002 to 0.8 °K, thereby suggesting a non-thermal mechanism of electrostimulation and electroporation.

At the same time, most studies with radiated ultra-wide band (UWB) pulses (0.3–20 ns, incident electric field strength in air up to 3.3 kV/cm) did not report any biological effect (see [11, 24] for review). Other studies reported weak and delayed effects of high-rate UWB trains, but no evidence of electrostimulation. The estimation of the free-field stimulation threshold yielded the electric field value of at least 12 kV/cm in air for a single 1-ns pulse, thereby explaining the negative findings with radiated UWB pulses [15]. The polarity reversal could also contribute to the reduced efficiency [4, 25] of radiated UWB pulses which are inherently bipolar.

Studies of bioeffects of sub-nanosecond duration EP remain essentially an uncharted territory. A single study with 800-ps pulses reported 50% lethality of B16 cells after the

delivery of 18,000 pulses at 150 kV/cm, or of 125 pulses at 950 kV/cm [9]. With 200-ps, 20–25 kV/cm pulses, lethal effects in B16 cells were observed only after at least 1.8 million pulses in combination with heating [10]. The same study reported a modest increase (10 pA) of a non-specific (leak) membrane current in NG108 cells after a minimum of 2000 pulses at estimated 20–40 kV/cm, which could also cause some heating.

The present study is the first trial of cell stimulation by sub-nanosecond EP. Using the mobilization of cytosolic Ca^{2+} as a sensitive endpoint of either VGCC opening or electroporation [4, 5, 17, 18, 22], we show that (1) 500-ps stimuli can open VGCC and elicit Ca^{2+} transients which last tens of seconds, (2) delivering multiple psEP enhances the effects, and (3) opening of VGCC cannot be explained by known mechanisms, such as heating from psEP stimulation or membrane depolarization by conventional electroporation or activation of VG Na^+ channels.

2. Materials and Methods

2.1. Cell culture

Chinese hamster ovary cells CHO-K1, a murine pituitary tumor GH3, and a murine neuroblastoma-rat glioma hybrid NG108 were obtained from the American Type Culture Collection (ATCC, Manassas, VA). They were propagated at 37 °C with 5% CO_2 in air according to the supplier's recommendations. CHO and GH3 cells were grown in Ham's F12K medium (Mediatech Cellgro, Herdon, VA) supplemented with either 10% fetal bovine serum (FBS) for CHO cells, or 2.5% FBS and 15% horse serum for GH3 cells. The media also contained 100 I.U./ml penicillin and 0.1 μg/ml streptomycin. NG108 cells were cultured in Dulbecco's Modified Eagle's medium (Caisson Labs, North Logan, UT) without sodium pyruvate, supplemented with 4 mM L-glutamine, 4.5 g/L glucose, 10% FBS, 0.2 mM hypoxanthine, 400 nM aminopterin, and 0.016 mM thymidine (without antibiotics). The media supplements were from Sigma-Aldrich (St. Louis, MO) except for the serum (Atlanta Biologicals, Norcross, GA). For the passage immediately preceding experiments, cells were transferred onto glass coverslips. For poorly adherent GH3 cells, the coverslips were coated with poly-L-lysine (Sigma-Aldrich). Cells were used in experiments after 12–24 hours of growing on the coverslips.

2.2. Calcium imaging

Detailed procedures employed for loading cells with Fura-2, dye calibration, and time lapse fluorescence imaging were reported previously [5]. To load the dye, cells on coverslips were incubated for 30 min in the physiological solution containing 5 μM of Fura-2/AM and 0.02% of Pluronic F-127 (Life Technologies, Grand Island, NY), in the dark at room temperature. The coverslips were rinsed in the physiological solution for 15 min and transferred into a glass-bottomed perfusion chamber (Warner Instruments, Hamden, CT) mounted on an IX71 inverted microscope (Olympus America, Center Valley, PA).

Unless indicated otherwise, all experiments were performed in a physiological solution containing (in mM): 140 NaCl, 5.4 KCl, 1.5 $MgCl_2$, 2 $CaCl_2$, 10 glucose, and 10 HEPES (pH 7.2, ~300 mOsm/kg). For Ca^{2+}-free conditions, $CaCl_2$ was replaced with 2 mM Na-EGTA; and for Na^+-free conditions, Na^+ was replaced with N-methyl-D-glucamine

(NMDG; all chemicals were from Sigma-Aldrich). When indicated in text, the solution contained 100 μM of L-type VGCC blocker verapamil and/or 1 μM of a wide-spectrum (N, P, and Q type) VGCC blocker ω-conotoxin MVIIC (Tocris Bioscience, Bristol, UK). Different solutions were changed by bath perfusion.

A fast wavelength switcher Lambda DG4 (Sutter Instruments, Novato, CA) was employed for dye excitation alternatively at 340 and 380 nm. Emission was measured at 510 nm every 150 ms (20 ms exposure at each wavelength) using a C9100-02 EM CCD camera (Hamamatsu Photonics, Japan). The cytosolic free Ca^{2+} concentration ($[Ca^{2+}]_i$) was calculated from Fura-2 emission ratio with Metafluor v.7.5 software (Molecular Devices, Sunnyvale, CA). Ca^{2+} measurements typically began one minute prior to psEP stimulation. In most experiments, Ca^{2+} traces were smoothed with a FFT filter utility of Origin 8.0 (OriginLab Corporation Northampton, MA).

2.3. Picosecond pulse stimulation and measurements

Previously described setup for nsEP delivery to selected individual cells [18, 30] was modified for psEP stimulation. Pulses of approximately 320 ps at 50% height were produced by an FPG 20-1 PM generator (FID GmbH, Burbach, Germany). Pulses were triggered externally and synchronized with image acquisitions by a TTL pulse protocol using Digidata 1440A board and Clampex v. 10.2 software (Molecular Devices). The exact timing of psEP delivery, pulse rate, and the number of pulses were all programmed in Clampex.

From the generator output the pulses were sent to a measurement tap and further to a 4 GHz, 20 Gs/s TDS7404 oscilloscope (Tektronix, Beaverton, OR), and to a π-network intended to absorb reflections from the load (Fig. 1A). The π-network consisted of several low-inductance carbon composition resistors housed in an aluminum hollow cylinder. The three equivalent resistances were 180 Ω, 64 Ω and 180 Ω and they acted as a 60 Ω absorber for pulses propagating in the 50 Ω coaxial cable. The space around the resistors was filled with silicone to prevent any high-voltage flashover. The π-network was calibrated by substituting the biological load with a high voltage 20X attenuator (142-NMFP-26, Barth Electronics, Boulder City, NV) and two 20-dB attenuators (Pasternack, Irvine, CA). The pulse after the π-network was almost identical in shape to the pulse measured from the D-dot sensor of the pulser (Fig. 1B). While the π-network provided impedance matching, it also attenuated the pulse by 8 dB, from 16 kV down to 6.2 kV. Because of the slight mismatch of the π-network to the coaxial cable (60 Ω to 50 Ω), we observed two post-pulse oscillations in about 30 ns after the main pulse, with amplitudes at least 10-fold smaller than the main pulse (not shown).

From the π-network, psEP were delivered to cells in the bath by means of a pair of tungsten rods (100 μm diameter, 170 μm gap) at the end of a 50-Ω RG316 coaxial cable (Fig. 1A). The connection was secured with epoxy, which also prevented the air breakdown between the rods. Down from the epoxy to the tips (3.5 mm), the rods were not insulated, and the air breakdown was avoided by submerging them into the solution.

The electrode assembly was driven by an MPC-200 robotic manipulator (Sutter Instruments, Novato, CA), to place the tips of the rods precisely at 50 μm above the coverslip surface

with selected cells being in the middle of the gap between the tips. The electric field values were determined by simulation with a 3D time-domain electromagnetic solver, CST microwave studio (Framingham, MA). These simulations also enabled taking into account the impedance discontinuities at the breakout of the coaxial cable and the transition from epoxy to the liquid medium. Instead of using the real waveform, in the simulation we applied a 320-ps Gaussian pulse to the input port the coaxial cable (Fig. 1C). To ensure the accuracy of the simulation, we used the analytical solution of the electric field inside the coaxial cable as a reference. The electric field between the two tungsten rods was also calibrated with the known analytical formula. The mesh size of the simulation was increased until the calculated field was stable and matched the analytical solution. For the peak voltage applied to the tungsten electrodes, the calculations were additionally validated using the Amaze 3D electrostatic solver (Field Precision, Albuquerque, NM). The difference of the electric fields for these two calculations was less than 10%. The voltage delivered to the stimulating electrodes was kept constant at 6.2 kV, which produced the electric field of 190 kV/cm at the position of cells (Fig. 1D).

The simulation also established broadening of the electric pulse due the impedance mismatch (Fig. 1C), to approximately 500 ps at 50% of the peak amplitude. Therefore we refer to the stimuli used in this study as being 500-ps pulses, despite the fact that the waveform measured at the output of the pulse generator was 320 ps.

2.4. Heating by psEP stimulation

Despite the sub-nanosecond pulse duration, high-rate trains of high-voltage psEP can cause considerable temperature rise. Accurate measurement of heating within the 170-μm gap between the electrodes, with a time resolution on the millisecond scale, is a challenging task and may alter the electric field [26]. The calculation of the temperature requires the solution of the heat equation:

$$\rho C\frac{\partial T}{\partial t}+\nabla\cdot(-k\nabla T)=\sigma(T)E^2 \quad [1]$$

where T is temperature, ρ is density of the medium, C is the specific heat capacity, k is the Boltzmann constant, σ is the electrical conductivity, and E is the electric field strength. Considering only the electric field in the center between the two electrodes, and neglecting any thermal losses due to diffusion and conduction (second term in equ. 1), equ. 1 is reduced to:

$$\rho C\frac{\partial T}{\partial t}=\sigma(T)E^2 \quad [2]$$

Disregarding small conductivity changes from heating of the medium (with a density of 1 g/cm^3 and a specific heat capacity of 4.2 J/gK [27]), the temperature rise for a single 500-ps, 190 kV/cm pulse with rectangular shape, will be less than 0.06 °C. For 100 pulses, neglecting thermal losses during the time between pulses, the temperature of the medium would rise by less than 6 °K. The actual temperature rise will be reduced by thermal diffusion into the less heated volume off-axis, and to the electrodes. In our case, this calculation of the upper limit of the temperature increase in the medium between the

electrodes signifies that while the effects of a single psEP and of brief trains (5–10 pulses) can be considered non-thermal, heating could potentially contribute to the bioeffect of longer trains. To limit heating, the maximum train duration for this study was 100 pulses.

3. Results

In our previous studies, CHO cells were chosen to study electroporation-induced Ca^{2+} transients with Fura-2 [5, 22]. The lack of VGCC expression in CHO cells makes electroporation the principal or the only mechanism for induction of Ca^{2+} transients by EP. The thresholds to elicit Ca^{2+} transients by nsEP were similar to those revealed by patch clamp and Tl^{+} uptake, arguably the most sensitive techniques for the detection of electroporation [20, 27]. However, 500-ps stimuli at 190 kV/cm, up to 100 pulses per train at either 200 Hz or 1 kHz, failed to elicit any Ca^{2+} response in CHO cells (n=117; data not shown). The lack of response in CHO cells suggested that psEP stimulation did not cause electroporation of the lipid phase of the cell membrane.

GH3 cells typically displayed random spontaneous Ca^{2+} oscillations of up to 300–500 nM in amplitude. On top of this activity, the delivery of a single psEP at 190 kV/cm caused a synchronized increase in Ca^{2+} level, either due to VGCC opening, or electroporation, or enhancement of the spontaneous oscillations by some other mechanism. The psEP-induced Ca^{2+} transient peaked at about 100 nM within 2–15 s after the stimulation, followed by a recovery to the basal level for about 100 s (Fig. 2A). Increasing the number of psEP (delivered at 1 kHz) increased the peak amplitude of the response, made its risetime shorter, and lengthened the recovery (Fig. 2A–C, E). The average amplitude of the Ca^{2+} transient increased only about 4-fold with increasing the number of psEP from 1 to 100. The response, even with 100 psEP, was reduced by at least 95% by pre-incubation of cells with an L-type VGCC blocker verapamil (Fig. 2D, E).

NG108 cells displayed essentially no spontaneous Ca^{2+} fluctuations. A single psEP triggered a minuscule (6+/−1.1 nM) but reproducible Ca^{2+} rise (Fig. 3A), and increasing the number of stimuli to 100 increased the response more than 100-fold (Fig. 3B,C,E). The psEP-induced Ca^{2+} transients could only partially by inhibited by either verapamil or ω-conotoxin, which could be explained by the fact that NG108 cells express multiple types of VGCC. Indeed, a cocktail of both inhibitors at high concentrations suppressed the transients by 85–100% (Fig. 3D,E).

The opening of VG Na^{+} channels in NG108 could potentially depolarize the cell membrane to activate VGCC. To test for the possible engagement of Na^{+} channels, we replaced external Na^{+} with a larger NMDG cation. Unexpectedly, this replacement caused a 5–10 fold increase of psEP-induced Ca^{2+} transients (Fig. 3E). While the lack of inhibition of Ca^{2+} transients rules out the role of VG Na^{+} channels in VGCC activation, the profound increase of the transients requires a separate explanation. NMDG has lower mobility in water than Na^{+}, which reduced the conductivity of the physiological solution approximately from 15 to 11 mS/cm. The reduced conductivity was reported to increase the effect of nsEP on cells in the solution, possibly by the transient electrodeformation (stretching) force that assumes its maximum value if cells are suspended in low-conductivity media [28]. However it is not

known if these findings and modeling are also applicable to sub-nanosecond pulses. Another feasible explanation is the inhibition of Na^+/Ca^{2+} exchanger in the absence of extracellular Na^+, which slows down the evacuation of Ca^{2+} from the cytosol and makes Ca^{2+} response larger and longer.

Similarly to GH3 cells, the recovery to basal Ca^{2+} level in NG108 cells typically took more than 100 s. While it could be a manifestation of a continued opening of VGCC, a more expected mechanism would be a slow function of pumps and other mechanisms responsible for Ca^{2+} buffering and removal. In order to test for the extended VGCC opening, we performed psEP stimulation in a Ca^{2+}-free medium, followed by the addition of external Ca^{2+} starting at 10 s after psEP (Fig. 4). In intact NG108 cells, the removal of extracellular Ca^{2+} decreased the cytosolic Ca^{2+} level by about 10 nM. Exposure of cells to psEP (190 kV/cm, up to 100 pulses at 1 kHz) in the absence of external Ca^{2+} did not elicit any response. However, superfusion with a medium containing 2 mM Ca^{2+} at 10 s after psEP revealed that the membrane was still permeable to Ca^{2+}, and the effect was proportional to the number of psEP applied. The data indicate that at least some VGCC remained open for at least 10 s after the stimulation. Notwithstanding slower VGCC inactivation in the absence of Ca^{2+}, this opening time is unusually long even for slow-inactivating VGCC [12, 29].

4. Discussion

The comparison of responses of CHO, GH3 and NG108 cells to psEP shows that the conventional lipid phase electroporation is probably not the principal mechanism for psEP-induced Ca^{2+} entry. The TMP required for poration ranges from 200 mV to 1 V for millisecond to microsecond pulses, and was reported to be even higher (1.4 V) for 60-ns EP [30]. Depending on the duration of electric pulses, the TMP increase relies on different mechanisms. For pulses longer than the membrane charging time (typically on the order of 100–1,000 ns) the TMP is increased by Maxwell-Wagner polarization. With reducing the pulse duration to values less than the charging time constant the applied electric field required for electroporation increases strongly [6]. For example, assuming a spherical cell with a diameter of 10 μm, a charging time constant of 100 ns, 1.4 V critical TMP value for electroporation (2.8 MV/cm applied to a 5-nm thick membrane), the amplitude of a 500-ps pulse required for electroporation will be 375 kV/cm. This amplitude may still be an underestimate since molecular dynamics models resulted in required sub-nanosecond membrane electric fields in excess of 5 MV/cm to generate pores [31, 32], which could only be reached with applied electric fields of over 650 kV/cm.

While the above calculations suggest that the amplitude of 190 kV/cm employed in this study could be vastly insufficient for electroporation by 500-ps pulses, we need to take into account that this pulse duration is in a transition zone between two coupling mechanisms, and the assumption that the membrane electric field is determined by the membrane charging process through ion currents might not be valid anymore. Provided that the pulse duration is shorter than the dielectric relaxation time of the cytoplasm ($\varepsilon_0\varepsilon_{cp}/\sigma_{cp}$), where ε_{cp} is the permittivity of the cytoplasm and σ_{cp} its conductivity [9], the electric field distribution in the cell is then increasingly determined by the cytoplasm and medium permittivities rather than their conductivities. Our pulse duration, 500 ps, is shorter than this time constant,

which is approximately 700 ps for ε_{cp}=80 and σ_{cp}=1 S/m, so the interaction of pulse and cell can likely be better described by the coupling of the electric field with dielectrics. Neglecting the effect of conduction currents, and considering only displacement currents, the electric fields at the interfaces from the medium to the membrane as well as the cytoplasm where dielectric stacking occurs, can be obtained by considering that the electric displacement ($D=\varepsilon_r\varepsilon_0 E$) is continuous in this case, i.e.,

$$\varepsilon_{r,water} E_{water} = \varepsilon_{r,mem} E_{mem} \quad [3]$$

where the membrane dielectric constant $\varepsilon_{r,mem}$ is approximately 10 [33, 34] and the dielectric constant $\varepsilon_{r,water}$ of medium and cytoplasm is about 80 (at 298 °K) [33]. The electric field in the membrane is therefore amplified by approximately a factor of 8 over the applied electric field (or, by other estimates [35], by a factor of 20). If we assume that the presence of cells on the coverslip does not perturb the field, the electric field strength at the cell position is calculated at 190 kV/cm (Fig. 1). It could produce 1.5–3.8 MV/cm in the membrane (resulting in TMP of 0.76–1.9 V over a 5 nm-thick membrane), which probably still is not high enough to cause lipid phase electroporation by a 500-ps pulse.

In summary, (a) the lack of response to psEP in CHO cells, (b) the induction of VGCC-dependent Ca^{2+} transients in other cells, and (c) the effective inhibition of such transients by specific VGCC blockers point to the activation of VGCC by psEP. Most importantly, VGCC opening occurred without detectable electroporation and apparently was not caused by the TMP loss due to the electroporative ion leakage. Then, what is the mechanism behind the change of the VGCC conformation from “closed” to “open”? The principal question is that the channel activation (i.e., the movement of the ion channel’s voltage sensor through several discrete intermediate conformation steps) takes 10–100 μs [12], which is 4–5 orders of magnitude longer than the membrane depolarization due the direct effect of psEP. As discussed above, the effects of psEP are defined by permittivity in the various parts of the cell rather than their conductivity, so the electric field acts directly on the membrane rather than causing its charging by the movement of ions [9]. Therefore, the induced TMP exists approximately for the duration of psEP itself, which is too short for VGCC opening in the standard fashion. Even if a modest charging component is present (because of slower low-amplitude components of psEP), it is difficult to explain how the membrane would hold this charge long enough to activate VGCC.

The phenomenon of opening of VG channels by EP several orders of magnitude shorter than the channel opening time is indicative of either a non-conventional membrane electroporation (where pores are so short-lived that usual methods of pore detection fail), or of a non-conventional mechanism of channel opening (e.g., by a direct effect of the applied field on the pore gate, bypassing the shift of the voltage sensor). A confirmation of either mechanism would have a significant impact on the understanding of cell membrane biophysics and on the development of the ultra-short pulse stimulation techniques.

Acknowledgments

The study was supported by R21EB016912 from NIBIB (to SX and AGP) and R01GM088303 from NIGMS (to AGP).

References

1. Neumann, E.; Sowers, AE.; Jordan, CA. Electroporation and Electrofusion in Cell Biology. Plenum; New York: 1989.
2. Pakhomov, AG.; Miklavcic, D.; Markov, MS. Advanced Electroporation Techniques in Biology in Medicine. CRC Press; Boca Raton: 2010. p. 528
3. Schoenbach, KH. Bioelectric effect of intense nanosecond pulses. In: Pakhomov, AG.; Miklavcic, D.; Markov, MS., editors. Advanced Electroporation Techniques in Biology in Medicine. CRC Press; Boca Raton: 2010. p. 19-50.
4. Pakhomov AG, Semenov I, Xiao S, Pakhomova ON, Gregory B, Schoenbach KH, Ullery JC, Beier HT, Rajulapati SR, Ibey BL. Cancellation of cellular responses to nanoelectroporation by reversing the stimulus polarity. Cell Mol Life Sci. 2014; 71:4431–4441. [PubMed: 24748074]
5. Semenov I, Xiao S, Pakhomov AG. Primary pathways of intracellular Ca(2+) mobilization by nanosecond pulsed electric field. Biochim Biophys Acta. 2013; 1828:981–989. [PubMed: 23220180]
6. Schoenbach KS, Hargrave B, Joshi RP, Kolb J, Osgood C, Nuccitelli R, Pakhomov AG, Swanson J, Stacey M, White JA, Xiao S, Zhang J, Beebe SJ, Blackmore PF, Buescher ES. Bioelectric Effects of Nanosecond Pulses. IEEE Transactions on Dielectrics and Electrical Insulation. 2007; 14:1088–1109.
7. Pakhomov AG, Gianulis E, Vernier PT, Semenov I, Xiao S, Pakhomova ON. Multiple nanosecond electric pulses increase the number but not the size of long-lived nanopores in the cell membrane. Biochim Biophys Acta. 2015; 1848:958–966. [PubMed: 25585279]
8. Napotnik TB, Wu YH, Gundersen MA, Miklavcic D, Vernier PT. Nanosecond electric pulses cause mitochondrial membrane permeabilization in Jurkat cells. Bioelectromagnetics. 2012; 33:257–264. [PubMed: 21953203]
9. Schoenbach KH, Xiao S, Joshi RP, Camp JT, Heeren T, Kolb JF, Beebe SJ. The effect of intense subnanosecond electrical pulses on biological cells. Ieee Transactions on Plasma Science. 2008; 36:414–422.
10. Xiao S, Guo S, Nesin V, Heller R, Schoenbach KH. Subnanosecond electric pulses cause membrane permeabilization and cell death. IEEE Trans Biomed Eng. 2011; 58:1239–1245. [PubMed: 21303739]
11. Molitor SC, Manis PB. Voltage-gated Ca2+ conductances in acutely isolated guinea pig dorsal cochlear nucleus neurons. Journal of neurophysiology. 1999; 81:985–998. [PubMed: 10085327]
12. Hille, B. Ionic Channels of Excitable Membranes. 3. Sinauer Associates; Sunderland, MA: 2001.
13. Jiang N, Cooper BY. Frequency-dependent interaction of ultrashort E-fields with nociceptor membranes and proteins. Bioelectromagnetics. 2011; 32:148–163. [PubMed: 21225892]
14. Nene D, Jiang N, Rau KK, Richardson M, Cooper BY. Nociceptor activation and damage by pulsed E-Fields. - art. no. 621904. Enabling Technologies and Design of Nonlethal Weapons. 2006; 6219:21904–21904.
15. Rogers WR, Merritt JH, Comeaux JA, Kuhnel CT, Moreland DF, Teltschik DG, Lucas JH, Murphy MR. Strength-duration curve for an electrically excitable tissue extended down to near 1 nanosecond. Ieee Transactions on Plasma Science. 2004; 32:1587–1599.
16. Wang S, Chen J, Chen MT, Vernier PT, Gundersen MA, Valderrabano M. Cardiac myocyte excitation by ultrashort high-field pulses. Biophysical journal. 2009; 96:1640–1648. [PubMed: 19217879]
17. Craviso GL, Choe S, Chatterjee P, Chatterjee I, Vernier PT. Nanosecond electric pulses: a novel stimulus for triggering Ca2+ influx into chromaffin cells via voltage-gated Ca2+ channels. Cell Mol Neurobiol. 2010; 30:1259–1265. [PubMed: 21080060]

18. Vernier PT, Sun Y, Chen MT, Gundersen MA, Craviso GL. Nanosecond electric pulse-induced calcium entry into chromaffin cells. Bioelectrochemistry. 2008; 73:1–4. [PubMed: 18407807]
19. Pakhomov, AG.; Pakhomova, ON. Nanopores: A distinct transmembrane passageway in electroporated cells. In: Pakhomov, AG.; Miklavcic, D.; Markov, MS., editors. Advanced Electroporation Techniques in Biology in Medicine. CRC Press; Boca Raton: 2010. p. 178-194.
20. Bowman AM, Nesin OM, Pakhomova ON, Pakhomov AG. Analysis of plasma membrane integrity by fluorescent detection of Tl(+) uptake. J Membr Biol. 2010; 236:15–26. [PubMed: 20623351]
21. Silve A, Leray I, Mir LM. Demonstration of cell membrane permeabilization to medium-sized molecules caused by a single 10 ns electric pulse. Bioelectrochemistry. 2012; 87:260–264. [PubMed: 22074790]
22. Semenov I, Xiao S, Pakhomova ON, Pakhomov AG. Recruitment of the intracellular Ca by ultrashort electric stimuli: The impact of pulse duration. Cell Calcium. 2013; 54:145–150. [PubMed: 23777980]
23. Vernier PT, Sun Y, Gundersen MA. Nanoelectropulse-driven membrane perturbation and small molecule permeabilization. BMC Cell Biol. 2006; 7:37. [PubMed: 17052354]
24. Seaman RL. Effects of exposure of animals to ultra-wideband pulses. Health Physics. 2007; 92:629–634. [PubMed: 17495665]
25. Ibey BL, Ullery JC, Pakhomova ON, Roth CC, Semenov I, Beier HT, Tarango M, Xiao S, Schoenbach KH, Pakhomov AG. Bipolar nanosecond electric pulses are less efficient at electropermeabilization and killing cells than monopolar pulses. Biochem Biophys Res Commun. 2014; 443:568–573. [PubMed: 24332942]
26. Pakhomov, AG. Practical Guide to High-Resolution Thermometry and Microdosimetry in Pulsed Electromagnetic Fields. In: Roach, WP., editor. Radiofrequency Radiation Dosimetry Handbook. 5. Directed Energy Bioeffects Division, Radio Frequency Radiation Branch; 2009. p. 69-100.www.dtic.mil/get-tr-doc/pdf?AD=ADA536009
27. Ibey BL, Xiao S, Schoenbach KH, Murphy MR, Pakhomov AG. Plasma membrane permeabilization by 60- and 600-ns electric pulses is determined by the absorbed dose. Bioelectromagnetics. 2009; 30:92–99. [PubMed: 18839412]
28. Muller KJ, Sukhorukov VL, Zimmermann U. Reversible electropermeabilization of mammalian cells by high-intensity, ultra-short pulses of submicrosecond duration. J Membr Biol. 2001; 184:161–170. [PubMed: 11719852]
29. Snutch, TP.; Peloquin, J.; Mathews, E.; McRory, JE. Molecular Properties of Voltage-Gated Calcium Channels. In: Zamponi, GW., editor. Voltage-Gated Calcium Channels. Landes Bioscience/Eurekah.com; Georgetown, TX, U.S.A: 2005. p. 61-94.
30. Frey W, White JA, Price RO, Blackmore PF, Joshi RP, Nuccitelli R, Beebe SJ, Schoenbach KH, Kolb JF. Plasma membrane voltage changes during nanosecond pulsed electric field exposure. Biophys J. 2006; 90:3608–3615. [PubMed: 16513782]
31. Vernier PT, Ziegler MJ, Sun Y, Gundersen MA, Tieleman DP. Nanopore-facilitated, voltage-driven phosphatidylserine translocation in lipid bilayers--in cells and in silico. Phys Biol. 2006; 3:233–247. [PubMed: 17200599]
32. Delemotte L, Tarek M. Molecular dynamics simulations of lipid membrane electroporation. J Membr Biol. 2012; 245:531–543. [PubMed: 22644388]
33. Camp JT, Jing Y, Zhuang J, Kolb JF, Beebe SJ, Song JH, Joshi RP, Xiao S, Schoenbach KH. Cell Death Induced by Subnanosecond Pulsed Electric Fields at Elevated Temperatures. Ieee Transactions on Plasma Science. 2012; 40:2334–2347.
34. Ermolina I, Polevaya Y, Feldman Y, Ginzburg B, Schlesinger M. Study of normal and malignant white blood cells by time domain dielectric spectroscopy. Ieee Transactions on Dielectrics and Electrical Insulation. 2001; 8:253–261.
35. Vernier, PT. Nanoscale Restructuring of Lipid Bilayers in Nanosecond Electric Fields. In: Pakhomov, AG.; Miklavcic, D.; Markov, M., editors. Advanced Elecroporation techniques in Medicine and Biology. CRC Press; Boca Raton, FL: 2010. p. 161-176.

Highlights

- 500-ps stimuli can open voltage-gated calcium channels
- Ca^{2+} transients elicited by ps stimuli last tens of seconds
- The opening of channels does not involve electroporation
- The data are indicative for an unconventional mechanism of channel opening

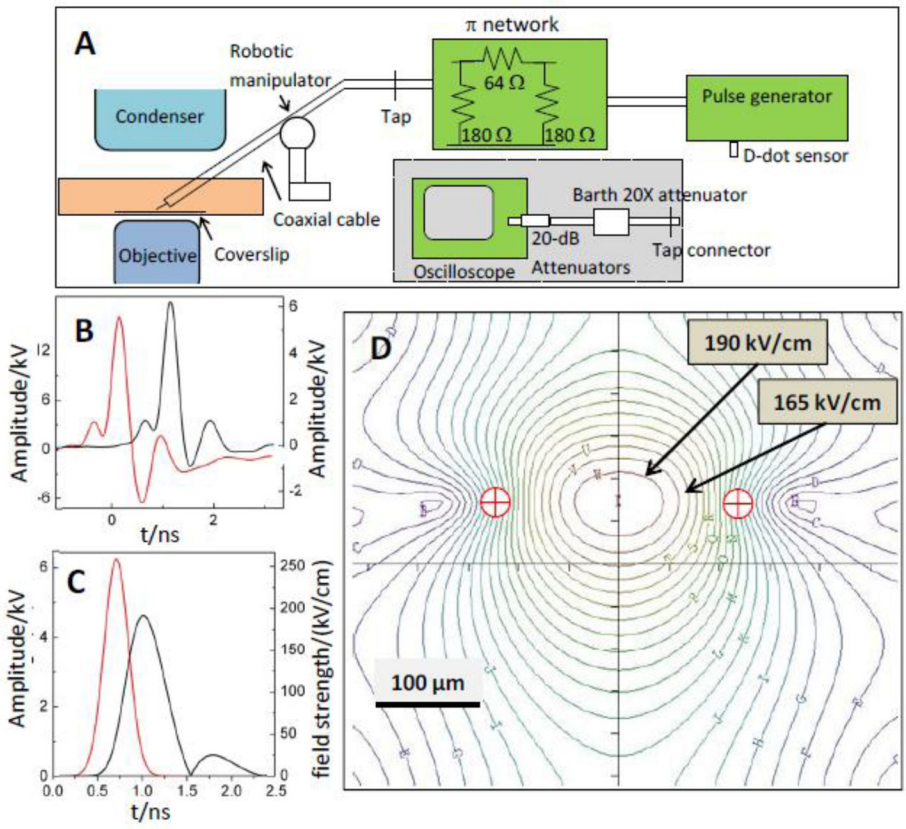

Fig. 1.

The picosecond pulse stimulation set-up and electric field characterization. (A) The overall schematic of the psEP stimulation system. (B) The waveform measured before the π network attenuator (red, left) and after it (black). The voltage scales on the left and right of the box correspond to the left and right waveforms, respectively. (C) A 320 ps Gaussian pulse that was used as a stimulus (red; left voltage scale) for pulse shape simulations and the resulting electric field pulse at the center of the cover slip (black; right scale). The electric pulse was broadened to 500 ps as measured at one half of its height. (D) The electric field strength distribution at the cover slip surface. The gap between the lowest points of two electrodes (marked by red target signs) and the coverslip was 50 µm. The stimulated cells were situated mostly within the central contour of the electric field (190 kV/cm). See text for more details.

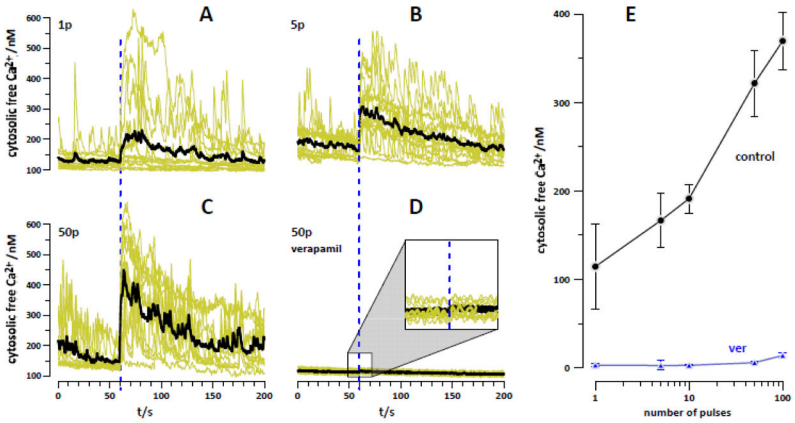

Fig. 2.

Effect of psEP stimulation in GH3 cells. (A–D) Calcium transients evoked by 1, 5, or 50 stimuli (1p, 5p, and 50p) at 190 kV/cm, 1 kHz. Shown are representative traces in individual cells (yellow lines, 15–25 cells per plot) and their average (black). Stimuli were delivered at 60 s into the experiment (vertical dashed lines). (D) Pre-treatment with verapamil inhibited the response to 50 psEP (a magnifier is used for better viewing). (E) Average peak amplitudes of the psEP-induced Ca^{2+} transient as a function of the number of pulses, in the physiological solution (control) and after pre-incubation with 100 μM verapamil (ver). Shown are mean values ± SE for 15–25 cells per group. The effect of verapamil is significant at $p<0.01$ (2-tailed *t*-test) for all datapoints.

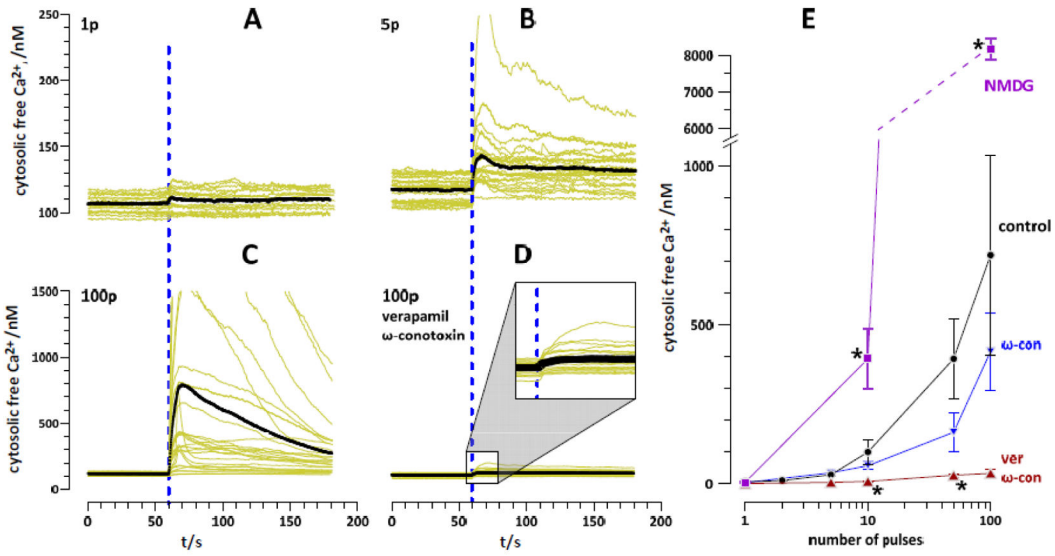

Fig. 3.

Effect of psEP stimulation in NG108 cells. (A–D) Calcium transients evoked by 1, 5, or 100 stimuli; designations are the same as in Fig. 2. Note different scales for A and B panels versus C and D panels; high-amplitude responses of some cells were clipped. (D) Pre-treatment with verapamil and ω-conotoxin inhibited the response to 100 psEP. (E) Average peak amplitudes of the psEP-induced Ca^{2+} transient as a function of the number of pulses, in the physiological solution (control); after pre-incubation with 1 μM ω-conotoxin ("ω-con") or 100 μM verapamil and 1 μM ω-conotoxin ("ver, ω-con"); and after the replacement of the external Na^{+} with NMDG ("NMDG"). Shown are mean values ± SE for 15 to 30 cells in most groups. * $p<0.01$ from the control (2-tailed *t*-test)

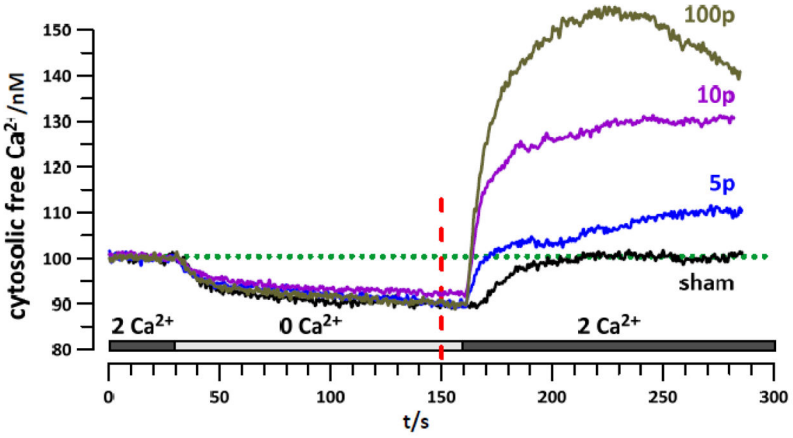

Fig. 4.

Stimulation by psEP in a Ca^{2+}-free solution does not elicit Ca^{2+} transients, but the delayed perfusion with 2 mM Ca^{2+} reveals its entry in psEP-treated cells. Shown are Ca^{2+} transients averaged from 12–18 cells. The bar above abscissa indicates the periods of perfusion with 0 and 2 mM external Ca^{2+}. Cells were stimulated by 5, 10, or 100 pulses (1p, 10p, and 100p; 190 kV/cm, 1 kHz) at 150 s (vertical dashed line). Sham-exposed cells were treated in the same manner, but no psEP were applied.